Elastic least squares reverse time migration

Linan Xu, Aaron Stanton and Mauricio D. Sacchi, Department of Physics, University of Alberta*

SUMMARY

While conventional migration is regarded as an approximation to the inverse of scattering using the adjoint operator, least squares migration is typically formulated as an iterative approach to estimate the reflectivity using forward and adjoint scattering operators. We provide a matrix based formulation of elastic scattering using a staggered-grid finite difference propagator, and derive its adjoint for use in elastic least squares Reverse Time Migration. We solve the system of equations via Conjugate Gradients with a Laplacian preconditioner that mitigates low frequency artefacts in the images.

INTRODUCTION

Converted wave processing methods typically treat data components as containing distinct wave modes. In isotropic media the vertical component contains the majority of the P-wave energy, while the radial component contains the majority of the S-wave energy. While this is the case for reflections originating from depth, shallow reflections or a complicated near surface may cause significant mixing of wave modes between data components.

A more robust treatment of multicomponent seismic data considers the vector nature of the data. In recent years there have been significant developments in vector processing methods for multicomponent seismic data, particularly in velocity analysis (Grandi et al., 2007), noise attenuation (Naghizadeh and Sacchi, 2012), wavefield separation (van Der Baan, 2006), and 5D interpolation (Stanton and Sacchi, 2013).

Elastic imaging methods have also been developed to handle vector wavefields. Chang and McMechan (1987) first introduced Elastic Reverse Time Migration (ERTM) to extrapolate isotropic P and S wavefields simultaneously. The method makes use of the two-way wave equation for the receiver side wavefields, but uses a one-way travel time based imaging condition with unseparated wavefields that can result in cross-talk artefacts. More recently, Yan and Sava (2008) and Yan and Sava (2009) developed angle gather based imaging conditions that separate source and receiver side wavefield potentials in isotropic and VTI media respectively.

While elastic migration offers an improvement over acoustic imaging, it fails to provide a true amplitude image because migration can be considered an approximation to inverse-scattering using the adjoint operator. Least squares migration (Nemeth et al., 1999), provides a means to more accurately recover an image of the subsurface and, with proper regularization, can be used to recover from acquisition noise, poor sampling of sources and receivers, and poor illumination of the subsurface. Recently Stanton and Sacchi (2015) extended least squares migration to the elastic case using one way wave equation migration. In this work we further extend elastic least squares migration to incorporate the two-way wave equation via Elastic Least-Squares Reverse Time Migration (ELSRTM).

In this work we stress that the exact adjoint is different from conventional migration (Chang and McMechan, 1987) and migration is a pseudo-adjoint to the forward operator, so it cannot pass the dot-product test (Claerbout, 1992). This property also exists in post-stack and pre-stack acoustic RTM (Ji, 2009) (Xu and Sacchi, 2016). In this research, we use a matrix-based formulation to derive the exact adjoint pair. It is an extension to the study of Xu and Sacchi (2016).

THEORY

Our primary goal in elastic imaging is to consider the interaction of compressional and shear modes between source and receiver-side wavefields. The relationship is expressed as reflectivity which is defined by the mode ratio

$$\tilde{m}_{(i,j)}(x,y) = \sum_t \frac{w_{r(i)}(x,z,t)}{w_{s(j)}(x,z,t)} \tag{1}$$

where $w_{s(i)}(x,z,t)$ is a synthetic source-side wavefield. The field is stimulated by a point source function at $\delta(x_s,z_s)src(t)$. Source energy spreads into the subsurface domain including reflector locations, $G(x,z|x_s,z_s)(\delta(x_s,z_s)src(t))$. The receiver wavefield is $w_{r(i)}(x,z,t)$. It consists of wave energy which is propagated from receiver locations into a half space in a time reversed sense. This process can be expressed as

$$G^*(x,z|x_r,z_r)(d(x_r,z_r,t)), \tag{2}$$

where * indicates backward propagation in time. It is obvious that, for the same wave modes, reflectivity can be considered as a ratio between incident and reflection wave energy. And for two different wave modes, reflectivity conveys mode conversion. In general, reflectivity can be treated as wave mode perturbation. Based on the Born approximation, the definition of reflectivity (1) can be utilized in the forward operator in ELSRTM.

$$d = G(x,z|x_s,z_s)\cdot\tilde{m}_{i,j}\cdot G(x,z|x_s,z_s)(\delta(x_s,z_s)src(t)) \tag{3}$$

As explained before, The combination of $G(x,z|x_s,z_s)(\delta(x_s,z_s)src(t))$ represents a wave-field which can be reshaped into a matrix form. The propagator $G(x,z|x',z')$ also can be expressed in a matrix formulation as will be explained in the next section. Now, the equation (3) is written in a matrix formulation as

$$\mathbf{d} = \mathbf{S_1}\cdot\mathbf{G}\cdot\mathbf{W_S}\cdot\tilde{\mathbf{m}}_{\mathbf{i,j}} = \mathbf{L}\tilde{\mathbf{m}}_{\mathbf{i,j}} \tag{4}$$

where $\mathbf{S_1}$ is a operator that samples wave energy at desired receiver locations, $\mathbf{S_2}$ is a spraying operator to apply reflectivity ($\tilde{\mathbf{m}}$) to each snapshot, and $\tilde{\mathbf{m}}_{i,j}$ is the model to be estimated. We define our cost function to be minimized as

$$J = \|\mathbf{LPa}-\mathbf{d}\|_2^2+\mu\|\mathbf{a}\|_2^2 \tag{5}$$

where $\mathbf{a}$ is the auxiliary variable $\mathbf{m} = \mathbf{Pa}$, μ is a trade-off parameter to control the level of data fitting, and $\mathbf{P}$ is a preconditioning operator. In this research, the $\mathbf{P}$ operator is an Laplacian operator to eliminate low wavenumber artefacts in the image. In least squares migration $\mathbf{L}$ is the de-migration (scattering) operator. The adjoint of it is recognized as the migration operator $\mathbf{L^T}$. In this research, the ELSRTM is solved by conjugate gradients which requires an exact adjoint pair of $\mathbf{L}$ and $\mathbf{L^T}$. The exact adjoint pair are derived from a matrix formulation, but applied programmatically.

In the time domain, the exact adjoint is the matrix transpose. Based on the forward operator, the perfect adjoint operator can be obtained by directly taking transpose to equation (6).

$$\mathbf{m_{i,j}} = \mathbf{S_1^T} \cdot \mathbf{W_S} \cdot \mathbf{G}^* \cdot \mathbf{d} = \mathbf{L^T d} \tag{6}$$

where $\mathbf{G}^*$ is a backward propagator in time and $\mathbf{S_1^T}$ is a summation operator which can be recognized as zero-lag cross-correlation. Therefore, the exact adjoint operator is consistent with a popular imaging condition commonly used in Reverse Time Migration (Claerbout, 1971). In the discrete domain, the time reversed propagation $\mathbf{G}^*$ is a pseudo-adjoint to forward propagation, but not the exact numerical adjoint. To derive the exact adjoint propagator, we start by writing the forward propagator in matrix form. In forward modelling, $\mathbf{G}$ is an operator to convert wave modes into particle velocities by Helmholtz decomposition ($\mathbf{H^{-1}}$), and solve the following five equations iteratively.

$$\frac{\partial v_x}{\partial t} = \frac{1}{\rho}\left(\frac{\partial \tau_{xx}}{\partial x} + \frac{\partial \tau_{xz}}{\partial z}\right) \tag{7}$$

$$\frac{\partial v_z}{\partial t} = \frac{1}{\rho}\left(\frac{\partial \tau_{zz}}{\partial z} + \frac{\partial \tau_{xz}}{\partial x}\right) \tag{8}$$

$$\frac{\partial \tau_{xx}}{\partial t} = (\lambda + 2\mu)\frac{\partial v_x}{\partial x} + \lambda \frac{\partial v_z}{\partial z} \tag{9}$$

$$\frac{\partial \tau_{zz}}{\partial t} = (\lambda + 2\mu)\frac{\partial v_z}{\partial z} + \lambda \frac{\partial v_x}{\partial x} \tag{10}$$

$$\frac{\partial \tau_{xz}}{\partial t} = \mu\left(\frac{\partial v_x}{\partial z} + \frac{\partial v_z}{\partial x}\right) \tag{11}$$

where v is particle velocity and τ is stress. Lame parameters are presented as λ and μ. The five equations are treated as a system and it is solved by finite difference on a staggered-grid with a Perfectly Matched Layer (PML) (Bérenger, 2007) boundary condition. The method consists of time stepping and space diffusion. In matrix form, the time stepping is

$$\begin{pmatrix} \mathbf{s}_1 \\ \mathbf{s}_2 \\ \vdots \\ \mathbf{s}_n \end{pmatrix}_f = \begin{pmatrix} \mathbf{I} & \cdots & \cdots & \mathbf{0} \\ \vdots & \ddots & & \vdots \\ \vdots & & \mathbf{I} & \vdots \\ \mathbf{0} & \cdots & \mathbf{FD} & \mathbf{FS} \end{pmatrix} \cdots \tag{12}$$

$$\begin{pmatrix} \mathbf{I} & \cdots & \cdots & \mathbf{0} \\ \mathbf{FD} & \mathbf{FS} & & \vdots \\ \vdots & & \ddots & \vdots \\ \mathbf{0} & \cdots & \cdots & \mathbf{I} \end{pmatrix} \begin{pmatrix} \mathbf{FS} & \cdots & \cdots & \mathbf{0} \\ \vdots & \mathbf{I} & & \vdots \\ \vdots & & \ddots & \vdots \\ \mathbf{0} & \cdots & \cdots & \mathbf{I} \end{pmatrix} \mathbf{H}^{-1} \begin{pmatrix} \mathbf{s}_1 \\ \mathbf{s}_2 \\ \vdots \\ \mathbf{s}_n \end{pmatrix}_i$$

where **FD** is a spatial diffusion operator and **FS** is the source injection matrix and $\mathbf{s}$ stands for snapshot. Each snapshot is a long column vector and consists of particle velocities and stress components. Then, **FD** and $\mathbf{s}$ multiplication are expressed as

$$\begin{pmatrix} \mathbf{v}_x' \\ \mathbf{v}_z' \\ \tau_{xx}' \\ \tau_{zz}' \\ \tau_{xz}' \end{pmatrix} = \begin{pmatrix} \mathbf{I} & \mathbf{0} & \mathbf{0} & \mathbf{0} & \mathbf{0} \\ \mathbf{0} & \mathbf{I} & \mathbf{0} & \mathbf{0} & \mathbf{0} \\ \mathbf{0} & \mathbf{0} & \mathbf{B}_4^{\tau_{xx}} & \mathbf{0} & \mathbf{0} \\ \mathbf{0} & \mathbf{0} & \mathbf{0} & \mathbf{B}_4^{\tau_{zz}} & \mathbf{0} \\ \mathbf{0} & \mathbf{0} & \mathbf{0} & \mathbf{0} & \mathbf{B}_4^{\tau_{xz}} \end{pmatrix} \begin{pmatrix} \mathbf{I} & \mathbf{0} & \mathbf{0} & \mathbf{0} & \mathbf{0} \\ \mathbf{0} & \mathbf{I} & \mathbf{0} & \mathbf{0} & \mathbf{0} \\ \mathbf{B}_2^{\tau_{xx}} & \mathbf{B}_3^{\tau_{xx}} & \mathbf{B}_1^{\tau_{xx}} & \mathbf{0} & \mathbf{0} \\ \mathbf{B}_2^{\tau_{zz}} & \mathbf{B}_3^{\tau_{zz}} & \mathbf{0} & \mathbf{B}_1^{\tau_{zz}} & \mathbf{0} \\ \mathbf{B}_3^{\tau_{xz}} & \mathbf{B}_2^{\tau_{xz}} & \mathbf{0} & \mathbf{0} & \mathbf{B}_1^{\tau_{xz}} \end{pmatrix} \begin{pmatrix} \mathbf{B}_4^{\mathbf{v_x}} & \mathbf{0} & \mathbf{0} & \mathbf{0} & \mathbf{0} \\ \mathbf{0} & \mathbf{B}_4^{\mathbf{v_z}} & \mathbf{0} & \mathbf{0} & \mathbf{0} \\ \mathbf{0} & \mathbf{0} & \mathbf{I} & \mathbf{0} & \mathbf{0} \\ \mathbf{0} & \mathbf{0} & \mathbf{0} & \mathbf{I} & \mathbf{0} \\ \mathbf{0} & \mathbf{0} & \mathbf{0} & \mathbf{0} & \mathbf{I} \end{pmatrix} \begin{pmatrix} \mathbf{B}_1^{\mathbf{v_x}} & \mathbf{0} & \mathbf{B}_2^{\mathbf{v_x}} & \mathbf{0} & \mathbf{B}_3^{\mathbf{v_x}} \\ \mathbf{0} & \mathbf{B}_1^{\mathbf{v_z}} & \mathbf{0} & \mathbf{B}_3^{\mathbf{v_z}} & \mathbf{B}_2^{\mathbf{v_z}} \\ \mathbf{0} & \mathbf{0} & \mathbf{I} & \mathbf{0} & \mathbf{0} \\ \mathbf{0} & \mathbf{0} & \mathbf{0} & \mathbf{I} & \mathbf{0} \\ \mathbf{0} & \mathbf{0} & \mathbf{0} & \mathbf{0} & \mathbf{I} \end{pmatrix} \begin{pmatrix} \mathbf{v}_x \\ \mathbf{v}_z \\ \tau_{xx} \\ \tau_{zz} \\ \tau_{xz} \end{pmatrix} \tag{13}$$

where $\mathbf{B}$ is a sub-matrix including all finite difference coefficients, PML coefficients and rock properties. Based on equation (12) and (13), we take the transpose of all matrices and sub-matrices, then the exact adjoint propagator is obtained. The matrix formulation is just a way to derive the adjoint. Instead of building giant matrices in memory, the forward and adjoint operator can be built up and implemented in computer codes by directly operating on matrix elements via indices.

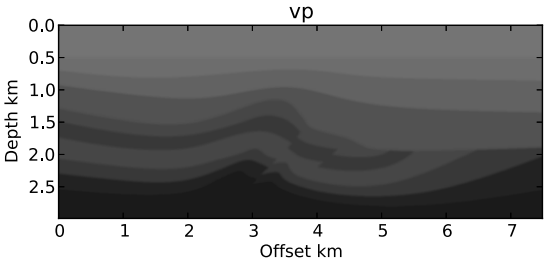

Figure 1: P-wave velocity model used for migration. The values range between 1500 m/s (light grey) to 3000 m/s (black). The S-wave velocity model is a scaled version of this model, and the density is constant at 1000 kg/m^3.

EXAMPLE

To test the effectiveness of the method we generated an elastic shot record at x=3600m using the velocity model shown

in figure 1. The spacing of the model is 10x10m with data sampled at 1ms in time. The modelled shot gather is shown in figure 5. For all calculations a 20th order finite difference stencil was used on the spatial axis. First we migrated the data using ERTM, producing the images shown in figure 3. The PP and PS images are dominated by low frequency artefacts. Next we applied 35 iterations of ELSRTM, producing the images shown in figure 4. As expected, least squares migration has mitigated the illumination of deeper reflectors and the Laplacian preconditioner has lessened the severity of the low frequency artefacts. Looking at the convergence (figure 2) and difference panels (figure 6) we find the algorithm has converged to an acceptable level of misfit (1.2%) given the fact that the input data are noise free.

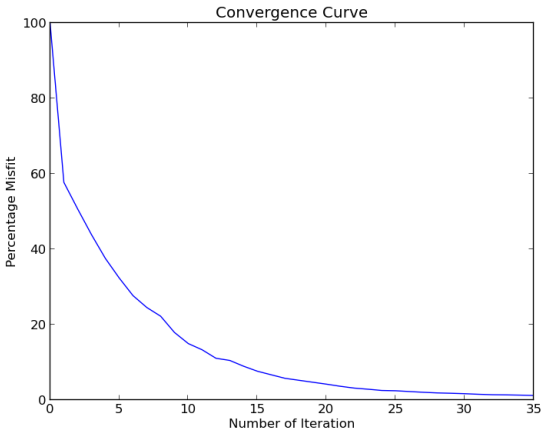

Figure 2: Percentage misfit of the estimated data versus the observed data as a function of iteration number.

CONCLUSIONS

We derived an elastic Born scattering operator and its adjoint using the two-way wave equation and applied it to Elastic Least Squares Reverse Time Migration (ELSRTM). To mitigate the effect of low frequency artefacts we preconditioned the problem using a Laplacian. The algorithm is able to improve the imaging of elastic data in the presence of acquisition noise, poor sampling of source and receivers, and poor illumination of the subsurface. As a next step in this research we plan to incorporate an angle gather imaging condition into the algorithm to better condition the inversion, and to allow for polarity corrections for multi-shot PS imaging.

ACKNOWLEDGEMENTS

We thank the sponsors of the Signal Analysis and Imaging Group (SAIG) for their support.

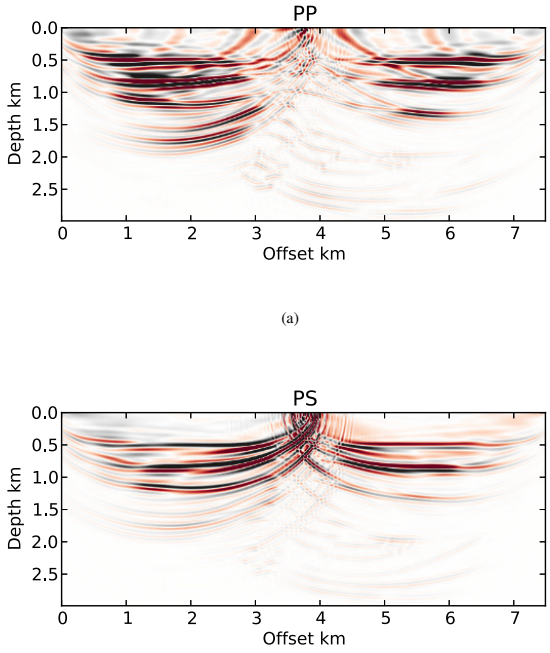

Figure 3: PP (a) and PS (b) images for 1 shot gather obtained via elastic RTM.

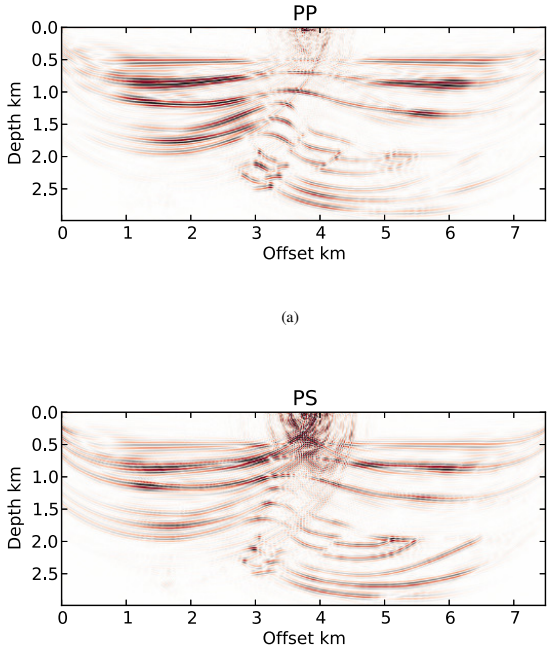

Figure 4: PP (a) and PS (b) images for 1 shot gather obtained via 35 iterations of ELSRTM.

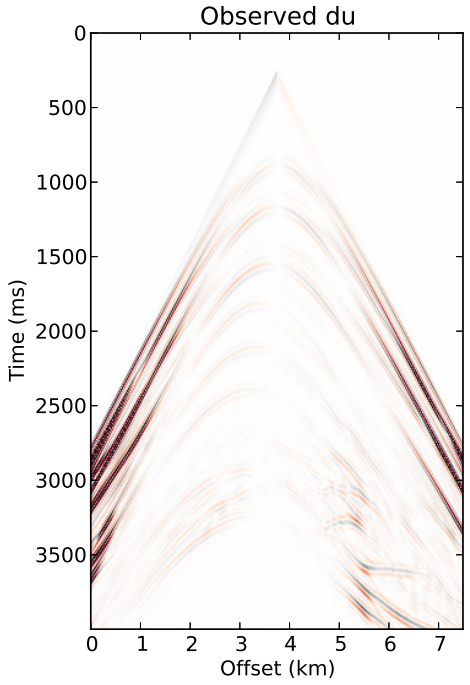

(a)

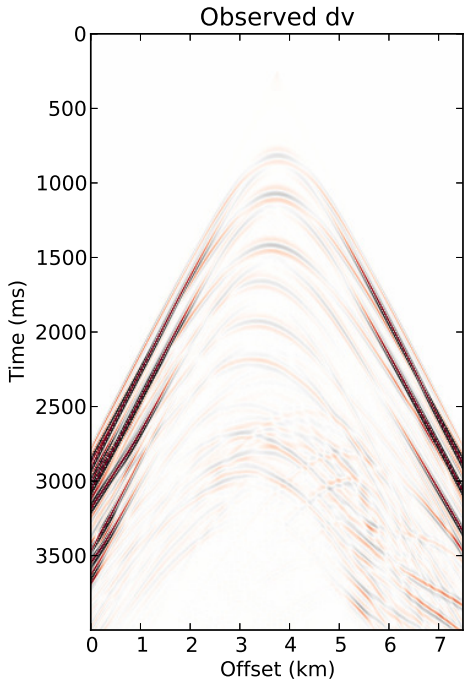

(b)

Figure 5: x (a) and z (b) data components for a finite difference synthetic shot gather at x=3600m.

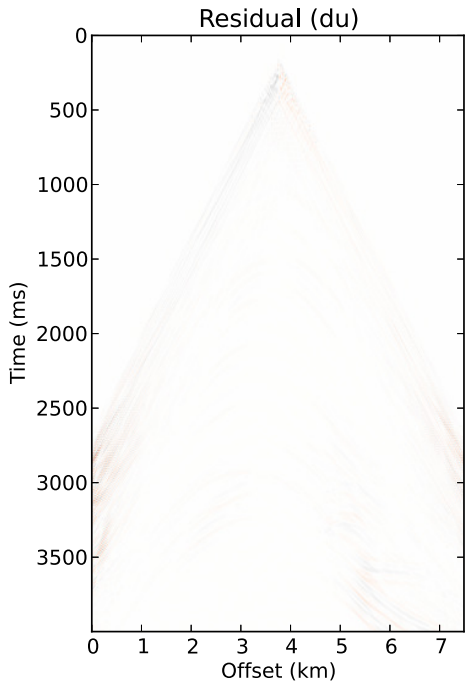

(a)

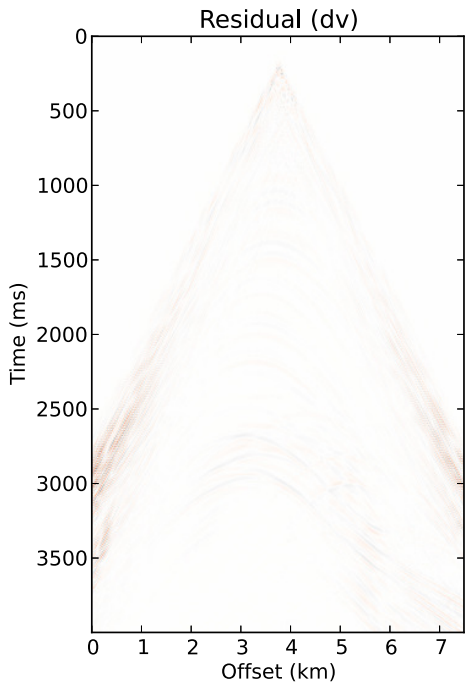

(b)

Figure 6: x (a) and z (b) component data residuals after 35 iterations of ELSRTM.

EDITED REFERENCES

Note: This reference list is a copyedited version of the reference list submitted by the author. Reference lists for the 2016 SEG Technical Program Expanded Abstracts have been copyedited so that references provided with the online metadata for each paper will achieve a high degree of linking to cited sources that appear on the Web.

REFERENCES

Bérenger, J.-P., 2007, Perfectly matched layer (pml) for computational electromagnetics: Synthesis Lectures on Computational Electromagnetics, **2**, 1–117, http://dx.doi.org/10.2200/S00030ED1V01Y200605CEM008.

Chang, W., and G. A. McMechan, 1987, Elastic reversetime migration: Geophysics, **52**, 1365–1375, http://dx.doi.org/10.1190/1.1442249.

Claerbout, J. F., 1971, Toward a unified theory of reflection mapping: Geophysics, **36**, 467–481, http://dx.doi.org/10.1190/1.1440185.

Claerbout, 1992, Earth sounding analysis: Processing versus inversion: Blackwell Scientific Publication.

Grandi, A., A. Mazzotti, and E. Stucchi, 2007, Multicomponent velocity analysis with quaternions: Geophysical Prospecting, **55**, 761–777, http://dx.doi.org/10.1111/j.1365-2478.2007.00657.x.

Ji, J., 2009, An exact adjoint operation pair in time extrapolation and its application in least-squares reverse-time migration: Geophysics, **74**, no. 5, H27–H33, http://dx.doi.org/10.1190/1.3173894.

Linan, X., and M. Sacchi, 2016, Least squares reverse time migration with model space preconditioning and exact forward/adjoint pairs: 78th Annual International Conference and Exhibition, EAGE, Expended Abstracts.

Naghizadeh, M., and M. Sacchi, 2012, Multicomponent f-x seismic random noise attenuation via vector autoregressive operators: Geophysics, **77**, no. 2, V91–V99, http://dx.doi.org/10.1190/geo2011-0198.1.

Nemeth, T., C. Wu, and G. T. Schuster, 1999, Least-squares migration of incomplete reflection data: Geophysics, **64**, 208–221, http://dx.doi.org/10.1190/1.1444517.

Stanton, A., and M. Sacchi, 2015, Least squares wave equation migration of elastic data: 77th Annual International Conference and Exhibition, EAGE, Expended Abstracts. http://dx.doi.org/10.3997/2214-4609.201412706.

Stanton, A., and M. D. Sacchi, 2013, Vector reconstruction of multicomponent seismic data: Geophysics, **78**, no. 4, V131–V145. http://dx.doi.org/10.1190/geo2012-0448.1.

van der Baan, M., 2006, Pp/pswavefield separation by independent component analysis: Geophysical Journal International, **166**, 339–348, http://dx.doi.org/10.1111/j.1365-246X.2006.03014.x.

Yan, J., and P. Sava, 2008, Isotropic angle-domain elastic reverse-time migration: Geophysics, **73**, no. 6, S229–S239, http://dx.doi.org/10.1190/1.2981241.

Yan, J., and P. Sava, 2009, Elastic wave-mode separation for vti media: Geophysics, **74**, no. 5, WB19–WB32, http://dx.doi.org/10.1190/1.3184014.